Cell PRESS
Neuron
Article

Early Increase in Extrasynaptic NMDA Receptor Signaling and Expression Contributes to Phenotype Onset in Huntington's Disease Mice

Austen J. Milnerwood,[1,2] Clare M. Gladding,[1,2] Mahmoud A. Pouladi,[2,3,4,6] Alexandra M. Kaufman,[1,2] Rochelle M. Hines,[1,2] Jamie D. Boyd,[1,2,5] Rebecca W.Y. Ko,[1,2] Oana C. Vasuta,[1,2] Rona K. Graham,[2,3,4,6] Michael R. Hayden,[2,3,4,6] Timothy H. Murphy,[1,2,5] and Lynn A. Raymond[1,2,*]
[1]Department of Psychiatry
[2]Brain Research Centre
[3]Centre for Molecular Medicine and Therapeutics
[4]Department of Medical Genetics
[5]Life Sciences Institute In Vivo Imaging Centre
University of British Columbia, Vancouver, BC V6T 1Z3, Canada
[6]Child and Family Research Institute, Vancouver, BC V6T 1Z3, Canada
*Correspondence: lynnr@interchange.ubc.ca
DOI 10.1016/j.neuron.2010.01.008

SUMMARY

N-methyl-D-aspartate receptor (NMDAR) excitotoxicity is implicated in the pathogenesis of Huntington's disease (HD), a late-onset neurodegenerative disorder. However, NMDARs are poor therapeutic targets, due to their essential physiological role. Recent studies demonstrate that synaptic NMDAR transmission drives neuroprotective gene transcription, whereas extrasynaptic NMDAR activation promotes cell death. We report specifically increased extrasynaptic NMDAR expression, current, and associated reductions in nuclear CREB activation in HD mouse striatum. The changes are observed in the absence of dendritic morphological alterations, before and after phenotype onset, correlate with mutation severity, and require caspase-6 cleavage of mutant huntingtin. Moreover, pharmacological block of extrasynaptic NMDARs with memantine reversed signaling and motor learning deficits. Our data demonstrate elevated extrasynaptic NMDAR activity in an animal model of neurodegenerative disease. We provide a candidate mechanism linking several pathways previously implicated in HD pathogenesis and demonstrate successful early therapeutic intervention in mice.

INTRODUCTION

NMDAR activity is imperative for vital brain functions, including synaptic plasticity, gene transcription, and cell survival (Bliss and Collingridge, 1993; Hardingham and Bading, 2003); however, overactivation of these receptors causes calcium overload and subsequent cell death (Arundine and Tymianski, 2003).

Evidence suggests that excessive NMDAR activity contributes to the pathogenesis of Huntington's disease (HD), a disorder characterized by degeneration of striatal medium-sized spiny neurons (MSNs; reviewed in Cowan and Raymond, 2006). Yet cognitive and psychiatric disturbances occur in HD gene carriers years before onset of motor symptoms or classical neuropathology (Duff et al., 2007; Solomon et al., 2007). Notably, NMDAR-dependent plasticity and transmission are altered in HD transgenic mice months prior to onset of motor deficits (Andre et al., 2006; Cepeda et al., 2001a; Li et al., 2004; Milnerwood et al., 2006; Milnerwood and Raymond, 2007; Van Raamsdonk et al., 2005), NR2B-containing NMDARs show increased surface expression, current, and toxicity in MSNs from HD mice (Fan et al., 2007; Shehadeh et al., 2006), and NR2B overexpression enhances striatal neuronal loss in HD mice (Heng et al., 2009). NMDARs are therefore an attractive candidate target for therapeutic intervention in HD. However, as these receptors are critical to many processes, broad intervention of NMDAR activity produces serious side effects (Chen and Lipton, 2006).

Neuronal culture studies demonstrate that the consequences of NMDAR activity are determined by the subcellular location of the receptor (reviewed in Hardingham and Bading, 2003; Köhr, 2006). A dichotomy between synaptic and extrasynaptic activity determines whether resulting signaling is beneficial (prosurvival) or detrimental (cell death pathways); synaptic activation promotes CREB phosphorylation, BDNF transcription, ERK activation, and antioxidant defense, whereas extrasynaptic signaling opposes synaptic signaling pathways in a dominant manner, leading to dendritic blebbing, mitochondrial breakdown, and cell death (Gouix et al., 2009; Hardingham et al., 2002; Leveille et al., 2008; Papadia et al., 2008). However, evidence for increased extrasynaptic NMDAR transmission in genetic models of human diseases has been lacking.

Here we present evidence indicating increased NR2B-containing extrasynaptic NMDARs in the striatum of transgenic mice expressing mutant full-length human huntingtin (htt) protein. Augmented extrasynaptic NMDAR signaling is detected at

ages preceding motor dysfunction and neuronal loss. Furthermore, HD mice treated with an NMDAR antagonist that preferentially targets extrasynaptic current (Leveille et al., 2008; Okamoto et al., 2009; Papadia et al., 2008) showed reversal of early nuclear signaling and motor learning deficits. The data provide a candidate mechanism for both early synaptic dysfunction, predicted to underlie cognitive deficits, and the delayed neuropathology observed in HD.

RESULTS

Yeast artificial chromosome (YAC) constructs are used to express the full human htt gene and its regulatory elements with normal (18) or pathological (72 or 128) CAG repeats in FVB/N mice. Similarly to human disease, YAC72/128 mice exhibit delayed neurodegeneration after cognitive and motor deficits (Hodgson et al., 1999; Slow et al., 2003; Van Raamsdonk et al., 2005). NMDAR activity is increased in MSNs from presymptomatic YAC72 and YAC128 mice (Fan et al., 2007; Milnerwood and Raymond, 2007; Zhang et al., 2008), and in cultured MSNs, mutant htt (mhtt) perturbs NMDAR surface trafficking (Fan et al., 2007). To assay NMDAR localization in MSNs of an intact network, we recorded evoked and spontaneous excitatory postsynaptic currents (e/sEPSCs) in acute slices using standard patch-clamp techniques (Milnerwood and Raymond, 2007). With the aim of developing strategies to prevent onset and progression of HD, we centered investigations on presymptomatic 1-month-old mice.

Strong Synaptic Stimulation Reveals Enhanced NMDAR Activity

In conditions designed to promote NMDAR activity at near-resting membrane potentials (−70 mV, low Mg^{2+} aCSF: 5 μM Mg^{2+}, 20 μM glycine), we evoked EPSCs (eEPSCs; local afferent stimulation) mediated by both NMDA and AMPA receptors (AMPAR), herein "dual" EPSCs. Evoked input-output curves showed no significant differences in dual eEPSC peak or charge between YAC18 and YAC128 MSNs (Figure S1). However, eEPSC charge relative to response peak increased with escalating stimulation, an effect more pronounced in YAC128 MSNs (Figure 1A, two-way ANOVA genotype $p = 0.002$, $F_{1,157} = 9.79$), significantly at high stimulation levels only (Mann-Whitney t test 250 μA $p = 0.03$). The data suggest that elevated NMDAR current in mhtt MSNs is only apparent in the slice at high levels of glutamate release and consequent spillover (Arnth-Jensen et al., 2002; Lozovaya et al., 2004; Scimemi et al., 2004). To directly test this, paired-pulse stimuli were delivered to increase presynaptic release (Figure 1B). Paired dual eEPSCs were recorded in the absence, then presence, of the NMDAR antagonist D-AP5, allowing calculation of I_{NMDA} by subtracting residual AMPAR current from initial AMPAR/NMDAR-mediated currents (Thomas et al., 2000).

Evoked field potential and AMPAR current amplitudes were not significantly different between YAC18 and YAC128 MSNs (Figure S1). In contrast, I_{NMDA} peak (Figure S1) and charge area were significantly elevated in YAC128 MSNs (Figure 1Bii, RM-ANOVA genotype $p = 0.006$, $F_{1,22} = 9.13$; interaction $p = 0.013$, $F_{1,22} = 7.31$), the source being significantly increased I_{NMDA} charge in YAC128 MSNs at high stimulation intensity. Relative charge ($I_{NMDA}C/I_{AMPA}$ peak) was also increased in YAC128 MSNs (genotype $p = 0.015$, $F_{1,22} = 6.89$). Direct comparisons revealed the source to be significant increases at high stimulation in the second (P2, facilitated) response. The results demonstrate that, in response to paired presynaptic stimuli, I_{NMDA} is 2- to 3-fold greater in YAC128 MSNs. Thus, augmented NMDAR activity is more readily observed with high levels of presynaptic release.

No Effect of Mutant htt on Spontaneous Synaptic NMDAR Activity

We also assayed I_{NMDA} at lower levels of presynaptic activity, as occur with spontaneous release (sEPSCs). In our coronal preparation, >90% of sEPSCs are action potential (AP) independent and likely due to spontaneous vesicle release (Figure S2); thus, sEPSC I_{NMDA} should represent NMDARs active directly under the release site, at the postsynaptic density (Figure 1Ci). I_{NMDA} was quantified in sEPSCs by subtractive calculation from dual currents (−70 mV, low Mg^{2+} aCSF). Strikingly, in the same cells that exhibited 2- to 3-fold increases in YAC128 NMDAR-mediated eEPSCs (with paired stimulation), YAC18 and YAC128 sEPSCs showed similar I_{NMDA} charge, relative charge (Figures 1Cii–1Civ), and decay constants (Figure S1). To investigate synaptic I_{NMDA} in standard ACSF (2 mM Mg^{2+}), we also unmasked I_{NMDA} by membrane depolarization (Figure 1D). Slowing of sEPSC decay constants was D-AP5 sensitive, and sEPSC decay measured at −20 mV was similar across all genotypes.

In contrast to paired-stimulus-evoked eEPSCs, sEPSCs may be biased toward a heterogeneous high probability of release (Pr) input pathway with a decreased NMDAR:AMPAR ratio, i.e., thalamostriatal versus corticostriatal inputs (Ding et al., 2008). If so, elevated I_{NMDA} in YAC128 paired-pulse eEPSCs may be attributable to increased contribution from corticostriatal connections; however, the high Pr thalamostriatal pathway has elsewhere been reported to exhibit an increased NMDAR:AMPAR ratio relative to the corticostriatal pathway (Smeal et al., 2008). In order to address such potential confounds, we increased Pr with the K^+ channel blocker 4-aminopyridine (4-AP, 100 μM, Cepeda et al., 2001b). This drug had no effect upon mEPSC frequency (Figure S2) but dramatically increased AP-dependent release (>4-fold increase in sEPSC frequency, Figure 2). Similarly to Figures 1B and 1C, we recorded before and after NMDAR block to calculate I_{NMDA} in mean events generated by sampling individual, large AP-dependent sEPSCs (detection threshold >35 pA). The mean amplitude and frequency of AP-dependent sEPSCs were indistinguishable (71.7 ± 4.7 pA, 65.1 ± 3.8 pA $p = 0.25$ and 7.2 ± 1.8 Hz, 6.6 ± 1.3 Hz $p = 0.82$ for YAC18 and YAC128, respectively) and subtracted I_{NMDA} peak, charge, and normalized charge were also similar between genotypes.

We also ruled out potential bias introduced by event sampling that may filter out important NMDAR activity, such as slow currents carried by NMDARs at AMPAR-silent synapses that lack sharp activation kinetics used to detect events. All-point histograms of 1 min sweeps in the absence and presence of NMDAR block were generated and group means compared (Figure 2iii). Such plots quantify both tonic (Gaussian fit) and

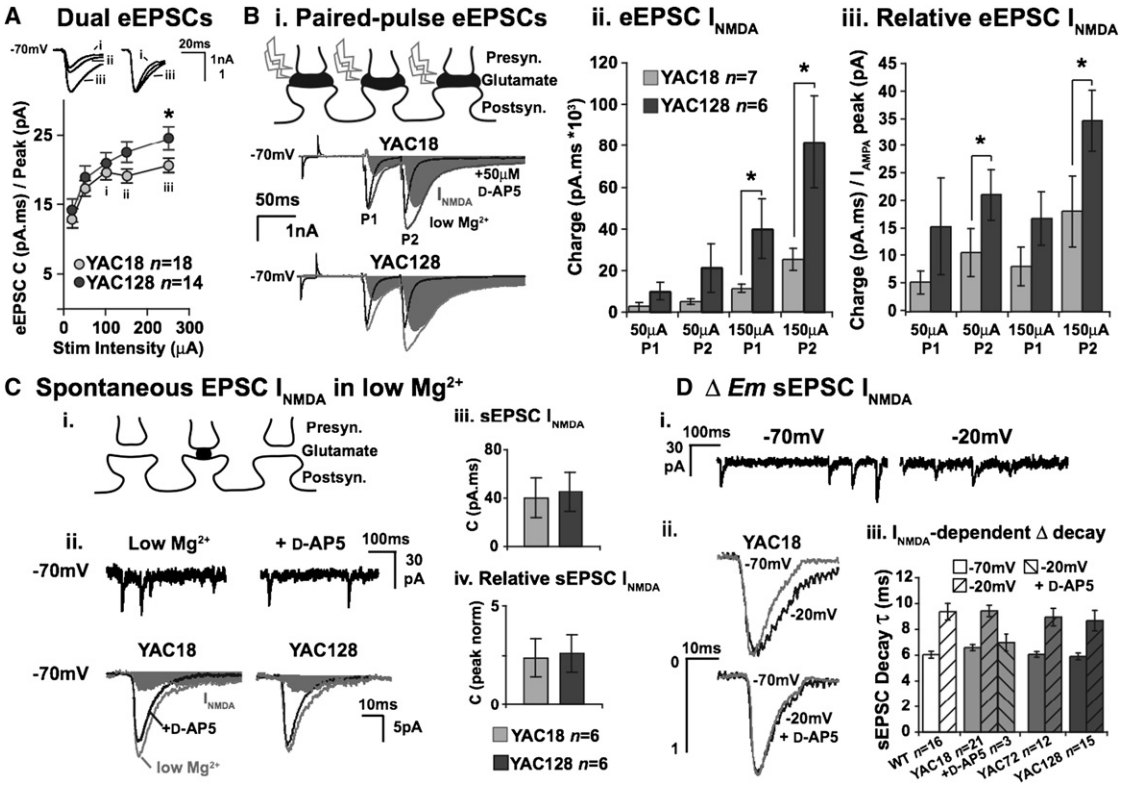

Figure 1. NMDAR Currents Are Increased in YAC128 MSNs but Only with High Levels of Presynaptic Release

(A) Dual AMPAR and NMDAR-mediated evoked EPSCs (eEPSCs, −70 mV low Mg^{2+}) produced by local glutamatergic afferent stimulation exhibit increased relative charge with increasing stimulus intensity (top left: Ai, Aii, Aiii = 100, 150, and 250 μA; top right: peak normalized); slowing is indicative of increased NMDAR contribution. YAC128 relative charge is greater with high-intensity stimulation (bottom).

(Bi) Cartoon depicting paired-pulse stimulation of afferents (strikes) resulting in high levels of action potential (AP)-dependent release at many synapses (top). Dual AMPA/NMDA-mediated eEPSCs in low Mg^{2+} (gray), +D-AP5 (I_{AMPA}, black). I_{AMPA} was subtracted from dual to give I_{NMDA} (fill). (Bii and Biii) I_{NMDA} charge (Bii) and relative charge (normalized to I_{AMPA}; Biii) are significantly increased in YAC128 (p, one-tailed t test).

(C) Cartoon depicting low-level spontaneous activity (Ci); AP-independent release occasionally occurs at single synapses, generating small sEPSCs (~20 pA, 2–3 Hz postsynaptically). Currents quantified as in (Bi); average sEPSC I_{NMDA} charge and relative charge (Cii–Civ; same cells as in B) are similar between genotypes.

(D) In standard aCSF, spontaneous currents (sEPSCs) have slower decay constants at −20 than −70 mV (Di and Dii), ΔTau (D-AP5-sensitive; I_{NMDA}-mediated) is similar across genotypes.

Data expressed as mean ± SEM.

phasic (shift from Gaussian) transmitter-dependent current (Glykys and Mody, 2007). There were no significant differences in dual or I_{AMPA} plots between genotypes, nor were there significant differences between genotypes in the magnitude of the NMDAR-dependent component.

The absence of any increase in sEPSC I_{NMDA}, even within large single events, together with 2- to 3-fold increased I_{NMDA} in large paired-pulse eEPSCs, suggests that elevated YAC128 I_{NMDA} is produced by glutamate spillover and activation of NMDARs outside the influence of individual release events, at peri- and/or extrasynaptic locations (Lozovaya et al., 2004).

Increased Extrasynaptic NMDAR Activation Unmasked by Augmented Glutamate Spillover

Precise connections between neurons are essential for discrete transmission, and synaptic fidelity is maintained by the action of glutamate uptake transporters on neurons and glia. In order to generate spillover to extrasynaptic receptors, we evoked isolated NMDAR EPSCs (standard aCSF, +60 mV, 10 μM CNQX) before and during application of the non-pump-reversing GLT-1 glutamate transport inhibitor DL-TBOA (10 μM, Figure 3A). TBOA promotes diffusion of glutamate from release sites and activation of NMDARs beyond the synaptic sphere of influence (Tzingounis and Wadiche, 2007).

In TBOA, NMDAR eEPSC kinetics slowed (Figure 3), in agreement with hippocampal studies (Arnth-Jensen et al., 2002; Scimemi et al., 2004). TBOA effects were reversible, and 88% ± 6% (n = 5) of eEPSC charge in TBOA was eliminated by D-AP5 (Figure 3Aiii). Slowing of I_{NMDA} was modest in WT and YAC18, occasionally pronounced in YAC72, and consistently pronounced in YAC128 MSNs. Both YAC128 I_{NMDA} Tau_W and peak normalized charge were significantly greater than WT or YAC18, with YAC72 showing intermediate values (Figure 3B, two-way RM-ANOVA interaction: Tau_W $p = 0.01$, $F_{4,62} = 3.5$,

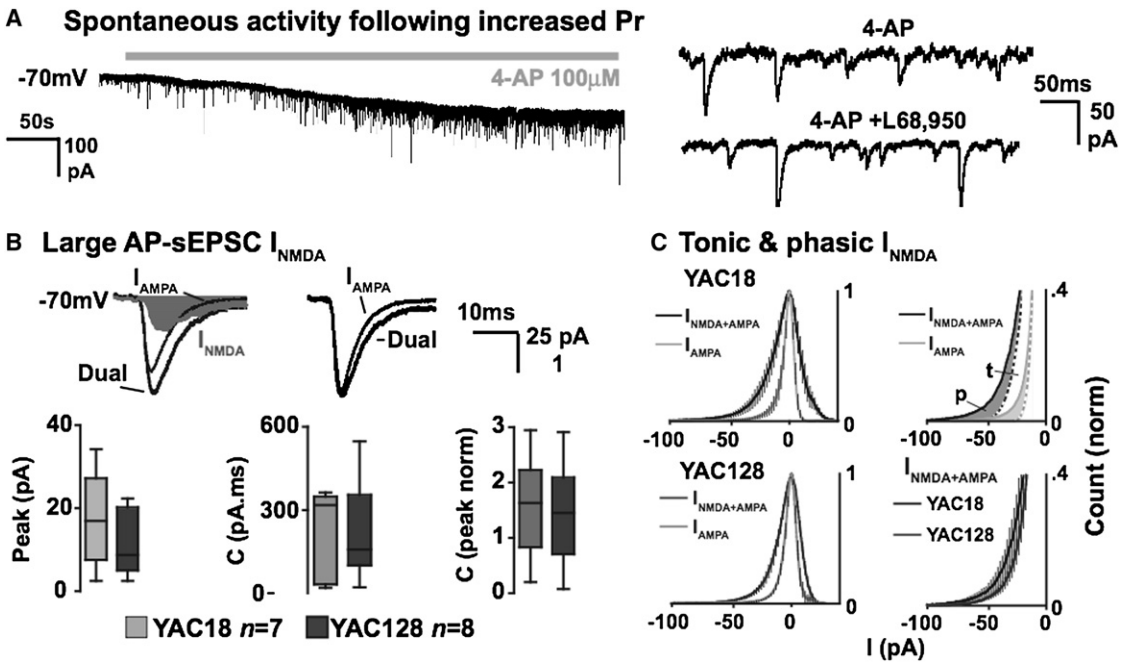

Figure 2. With Elevated Pr, sEPSC and Tonic I_{NMDA} Are Similar

(A) After increasing Pr (100 μm 4-AP), NMDAR activity was assessed by NMDAR block (right; 5 μM L689,560).

(B) AP-dependent dual sEPSCs (>30 pA) were averaged for each cell as in Figures 1B and 1C; there were no differences in I_{NMDA} peak, charge, or relative charge (following peak normalization, right) between genotypes.

(C) To avoid event sampling bias, all-point histograms ±I_{NMDA} were produced for each cell, and group means were compared to quantify both tonic (Gaussian fit) and phasic (negative shift from Gaussian) glutamatergic activity (expanded top right). Dual I_{NMDA}/I_{AMPA} and I_{AMPA} current distributions (top and bottom left) were similar between genotypes, as was the difference between the two histograms within genotype (I_{NMDA}). Bottom right: expanded dual I_{NMDA}/I_{AMPA} plot shows that phasic I_{NMDA} activity is not increased, but reduced in YAC128s.

Data expressed as mean ± SEM, excepting whisker plots in (B).

normalized charge p = 0.001, $F_{4,62}$ = 5.2, Bonferroni post test). The data suggest extrasynaptic I_{NMDA} (Ex-I_{NMDA}) charge transfer was 2- to 3-fold increased in YAC128, and increased intermediately in YAC72, MSNs. Consistent with these findings, TBOA also increased the holding current (I_{hold}), a portion of which is NMDAR-dependent (Le Meur et al., 2007). NMDAR-dependent increases in I_{hold} over the first 5 min of TBOA exposure were significantly greater in YAC128 MSNs (Figure S3). Thus, the results of TBOA exposure are also consistent with a mhtt-dependent increase in the number, or activity, of extrasynaptic NMDARs.

Elevated Extrasynaptic NMDAR Signaling Requires Caspase-6 Cleavage of mhtt

There is considerable evidence for caspase cleavage of htt in HD pathogenesis (Wellington et al., 2000). Notably, C6R mice express a construct identical to YAC128 mice, excepting a point mutation rendering mhtt resistant to caspase-6 cleavage. C6R mice are resistant to the excitotoxicity, neurodegeneration, and behavioral characteristics of YAC128 mice (Graham et al., 2006a; Pouladi et al., 2009), strongly arguing that mhtt proteolysis is required for the formation of toxic htt fragments. However, electrophysiological investigation of C6R mice has not previously been presented. Here, we found that C6R MSNs were remarkably similar to YAC18 and WT MSNs; increases in I_{NMDA} decay, charge, and I_{hold} following TBOA application were modest and significantly different from YAC128 MSNs (Figures 3B and S3). The data suggest that caspase-6 cleavage of mhtt is necessary for increased Ex-I_{NMDA}, subsequent behavioral deficits, excitotoxicity, and neurodegeneration.

Elevated Ex-I_{NMDA} Occurs Independently of Synaptic NMDAR Activation

To further characterize Ex-I_{NMDA}, we ruled out the possibility that increased I_{NMDA} in TBOA may be attributable to modulation of synaptic NMDARs. Following blockade of synaptic I_{NMDA} with the use-dependent, irreversible antagonist MK-801 and subsequent washout, we found that TBOA resulted in a highly significant elevation of Ex-I_{NMDA} in YAC128 MSNs (Figure 4). Notably, concomitant I_{AMPA} and field potentials were reduced, indicating that TBOA did not increase glutamate release. The data demonstrate that elevated YAC128 I_{NMDA} is not carried by altered synaptic responses.

Elevated Ex-I_{NMDA} without Dendritic Morphological Alteration and Persistence with Age

Differential synaptic development or other alterations to MSN morphology already present at 1 month may contribute to the observed increased Ex-I_{NMDA}. However, Golgi impregnation and 3D reconstruction of YAC18 and YAC128 MSNs revealed

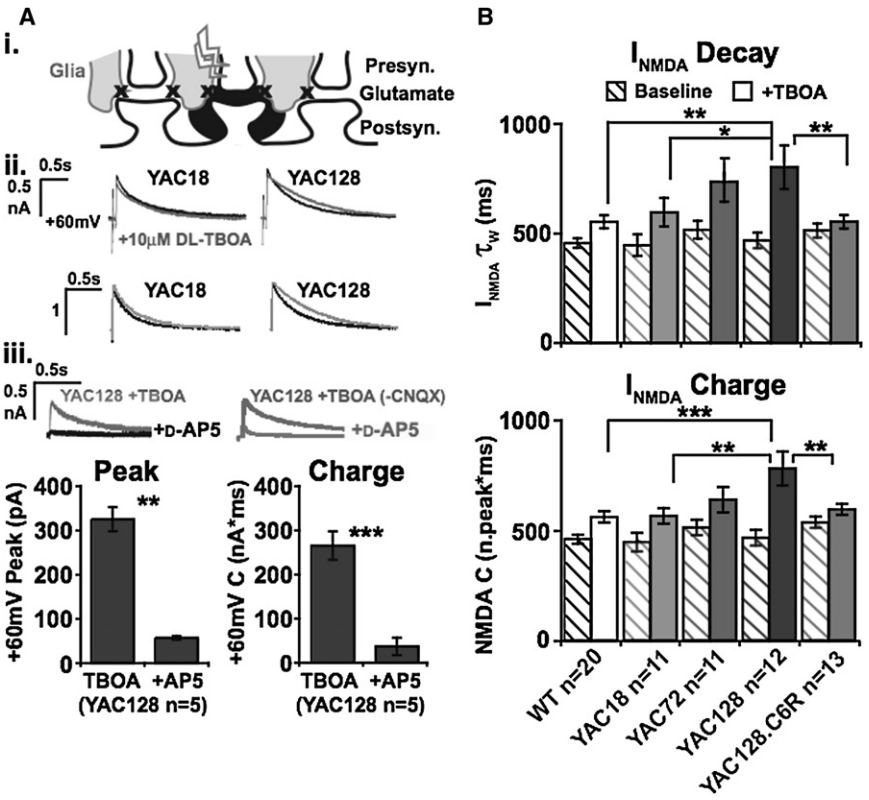

Figure 3. Glutamate Transport Block, Increased Spillover, and Elevated Extrasynaptic NMDAR Activity in YAC128 MSNs

(Ai) Cartoon depicting increased glutamate diffusion from the synaptic cleft following stimulation in the absence of glial glutamate reuptake. (Aii) Representative isolated NMDAR eEPSCs (standard aCSF, +60 mV, 10 μM CNQX top, peak scaled below) showing pronounced slowing of I_{NMDA} by DL-TBOA (10 μM TBOA, 10 min). (Aiii) Slower eEPSCs in TBOA are entirely NMDAR mediated; peak and charge are much reduced by AP5 (paired t test).

(B) Top: TBOA produces a significantly greater slowing of YAC128 I_{NMDA} that is entirely reversible (see text). Bottom: I_{NMDA} charge (peak scaled) is significantly increased in YAC128s following TBOA application (two-way RM-ANOVA Bonferroni post hoc).

Data expressed as mean ± SEM.

no significant differences in Sholl analysis, dendritic number, endpoints, branching, total length, or spine densities between genotypes (Figure 5A).

To determine whether elevated Ex-I_{NMDA} is observed in aged mice, after phenotype onset, we recorded in slices from mice aged >1 year. Although at 12 months YAC128 mice show 18% striatal cell loss (Slow et al., 2003), all surviving cells exhibited inward rectification characteristic of MSNs and membrane properties indistinguishable from age-matched WT littermates (Figure 5B). As at 1 month, at ≥1 year eEPSC relative charge was increased, but only at high stimulus intensities (two-way RM ANOVA interaction p = 0.04, $F_{2,22}$ = 3.6, direct comparison MW t test), and TBOA resulted in significantly increased Ex-I_{NMDA} (two-way RM ANOVA interaction p = 0.03, $F_{1,6}$ = 7.7, direct comparison MW t test).

Aside from alterations to MSN morphology, a loss of glial contacts could also produce increased glutamate diffusion and elevated Ex-I_{NMDA}. Ultrastructural assessment (Figure 5C) revealed no difference between WT and YAC128 (p = 0.5, 0.76 ± 0.06, 0.82 ± 0.04, respectively) in the proportion of asymmetric synapses with contacting astrocytes, and there were no differences in the distance between astrocytic processes and the postsynaptic density (PSD, p = 0.07, 70.8 ± 6.6 and 83.4 ± 6.9 nm).

Elevated Ex-I_{NMDA} Is NR2B Dependent

In order to avoid other potential developmental confounds, at 1 month we assayed YAC128 versus WT littermates. Further, we increased the concentration of TBOA (from 10 to 30 μM, also see Figure 4), to control for differences in transporter efficacy. As before, eEPSC relative charge was significantly increased in YAC128 MSNs only at high stimulus intensities (Figure 6A, two-way ANOVA genotype p = 0.009, $F_{1,63}$ = 7.1, direct comparison t test). Transient TBOA application (30 μM) led to a fully reversible 50% increase in WT I_{NMDA}, in contrast to a 125% increase in YAC128 I_{NMDA} (Figures 6B and 6C, two-way ANOVA genotype p = 0.0001, $F_{1,60}$ = 34.6, Boferroni post hoc), demonstrating that deficits in transporter efficacy are unlikely to underlie augmented Ex-I_{NMDA} in YAC128 mice.

Next we investigated a role for NR2B-type NMDARs and mGluRs in elevated Ex-I_{NMDA}. The NR2B NMDAR subunit-selective antagonist ifenprodil (10 μM; Williams, 2001) produced small reductions in I_{NMDA} peak in both WT and YAC128 MSNs (Figure 6D, 16.7% ± 4.3% p = 0.01 and 19.7% ± 3.4% p = 0.02, respectively, paired t test). Upon subsequent transient application of TBOA, ifenprodil eliminated the difference between YAC128 and WT I_{NMDA} decay Tau_W (Figures 6E and 6F, p = 0.6). Contrastingly, the broad spectrum group I/II mGluR antagonist S-MCPG (250 μM; Sergueeva et al., 1993) had no significant effect upon TBOA-induced increase in Ex-I_{NMDA} TauW in WT or YAC128 MSNs (Figure 6F), demonstrating that mGluR activity is not required. Collectively, the data suggest that elevated Ex-I_{NMDA} in YAC128 MSNs is carried by a distinct extrasynaptic population of NR2B-containing NMDARs.

Altered Subcellular Localization of NMDAR Subunits

To determine whether synaptic NMDAR trafficking is altered by mhtt expression, we investigated subunit localization by fractionation of synaptosomes (Pacchioni et al., 2009). Synaptosome preparations contain pre- and postsynaptic structures (reviewed in Whittaker, 1993); including endosomal, perisynaptic, extrasynaptic membranes, and the specialized postsynaptic

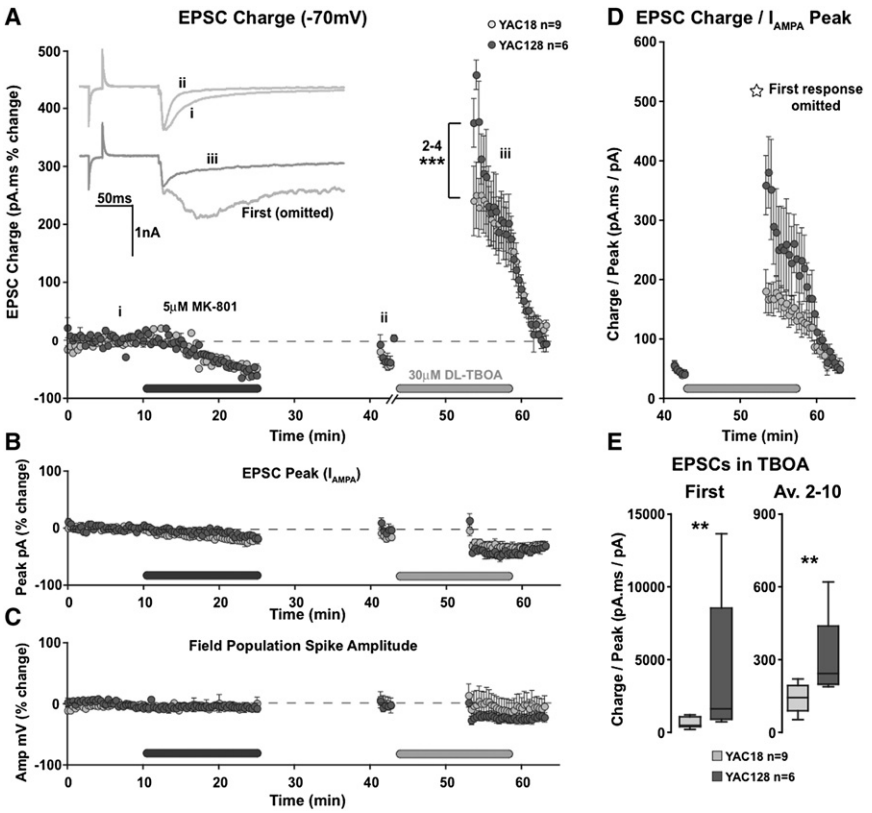

Figure 4. Block of Synaptic I_{NMDA} and Elevated TBOA-Induced Ex-I_{NMDA} in YAC128 MSNs

(A) MK-801 (5μM) irreversibly blocked I_{NMDA} components of "dual" eEPSCs (Ai and Aii), while preserving I_{AMPA} (for assessment of preparation stability).

(B and C) After a period of quiescence for MK801 wash-out, irreversible block is demonstrated by persistent loss of slow I_{NMDA} (ii, I_{AMPA} persists; B and C, last datum renormalized). Application of TBOA (30 μM, 10 min) results in re-emergence and augmentation of I_{NMDA} upon resumption of test shocks (iii), reflecting peri/extrasynaptic NMDAR activity (Ex-I_{NMDA}). This reversible effect is significantly greater in YAC128s (second through fourth shocks upon resumption, two-way ANOVA genotype $p = 0.0005$ $F_{2,39} = 14.3$).

(D) YAC128 relative I_{NMDA} charge is >2-fold increased following peak (I_{AMPA}) normalization to account for reductions in presynaptic release, suggested by subtle alterations in fields and I_{AMPA} peak (B and C).

(E) Quantification of first and next nine averaged responses after resumption of stimulation in TBOA in (D); YAC128 relative charge was significantly increased (Mann Whitney t tests; first response $p = 0.007$, 2–10 average $p = 0.005$).

Data expressed as mean ± SEM, except for the whisker box plots in (E).

density (PSD). Further digestion of synaptosomes yields an insoluble "PSD-enriched" membrane fraction and a "non-PSD enriched" membrane fraction, which includes extrasynaptic plasma membrane receptors (Figure 7A). A clear separation of PSD and non-PSD membranes was achieved, as demonstrated by the distribution of PSD-95, synaptophysin, calnexin, and Rab5 (Figures 7A and S4). NR1, NR2A, and NR2B immunoreactivity was significantly increased in YAC128 striatal "non-PSD" fractions with respect to YAC18 (12.5 ± 4.9 $p = 0.01$, 15.5 ± 3.4 $p = 0.03$, and 48.3% ± 13.2% $p = 0.002$, respectively, Wilcoxon SR test; Figure 7A). All three subunits were also decreased in the synaptic "PSD" fraction, although this reduction only reached significance for NR2B (−15.5% ± 5.0% $p = 0.02$). A similar pattern was also observed in non-PSD fractions from cortical tissue, with significant increases in NR1 and NR2B subunits (12.5 ± 4.8 $p = 0.02$ and 59.6% ± 30.1% $p = 0.02$, respectively). Unlike the striatum, there were no reductions in NMDAR subunit immunoreactivity in cortical PSD fractions.

Memantine Treatment Restores CREB Activation and Motor Learning

The mislocalization of NMDAR subunits to peri- and extrasynaptic membranes and associated increases in Ex-I_{NMDA} would be predicted to dominantly oppose synaptic NMDAR nuclear signaling, reducing CREB activation (Hardingham et al., 2002). We therefore assayed basal CREB activity in nuclear fractions of YAC18 and YAC128 striatum from mice aged 1 month (Figure 7B). As predicted, there was significantly less nuclear CREB activity in YAC128 striatum ($p = 0.04$ MW t test).

Remarkably, in a recent study low-dose treatment with the weak NMDAR antagonist memantine from 2 months reversed neuropathological and behavioral deficits in YAC128 mice when assessed at 12 months (Okamoto et al., 2009). Furthermore, high-dose memantine was detrimental to YAC128 mice, consistent with in vitro observations demonstrating that low-dose memantine preferentially antagonizes deleterious extrasynaptic NMDAR activity and signaling (Leveille et al., 2008; Okamoto et al., 2009; Papadia et al., 2008). We compared nuclear CREB activity in the striatum of 4-month-old WT and YAC128 mice with YAC128 mice that received 1 mg/kg (low dose) memantine from 2 months (Figure 8A). There were significant effects of genotype and treatment, due to the predicted reduction in nuclear CREB activation in the YAC128 striatum versus WT controls, and a striking reversal of this early deficit in the memantine-treated mice.

At 2–4 months of age, although free of obvious motor dysfunction, YAC128 motor learning is impaired, as evidenced by increased failures (number of falls) when learning the rotarod test (Van Raamsdonk et al., 2005). Here, we observed similar results and, in addition to reversing the CREB signaling deficit, memantine treatment significantly reversed this early motor learning deficit (Figure 8B). These data add to the previous report of rescue of motor function in YAC128 at 12 months of age (Okamoto et al., 2009) and demonstrate that appropriate early therapeutic intervention produces a significant alleviation of phenotype onset and progression of HD.

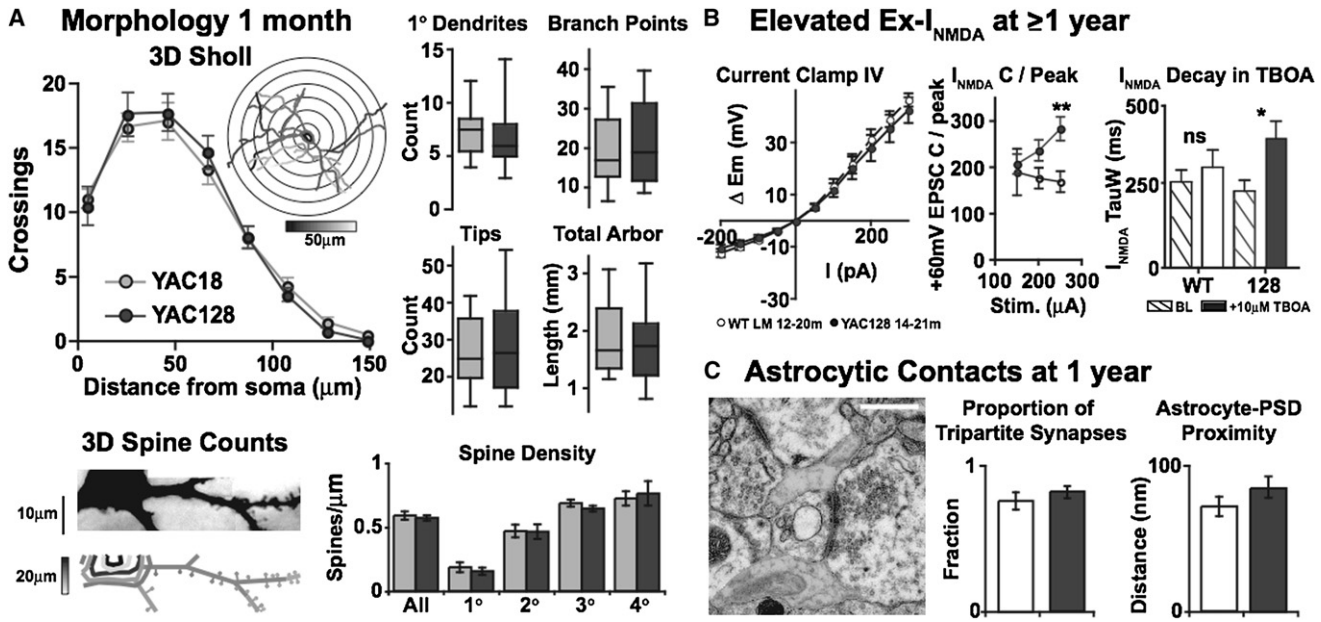

Figure 5. Elevated Ex-I_{NMDA} Is Not Attributable to Altered Morphology or Reduced Glial Contact and Persists in Aged YAC128s

(A) Golgi impregnation of 1 month YAC18 and YAC128 brains. Top: 3D cell reconstruction and Sholl analysis demonstrated no significant differences in MSN morphology (YAC18 n = 20, YAC128 n = 19). Bottom: Photomontage and example of 3D reconstructed spines (left); densities were similar between genotypes in 1°, 2°, 3°, and 4° dendrites (YAC18 n = 13, YAC128 n = 13).

(B) WC patch recordings in YAC128 (filled) and aged-matched wild-type littermates (clear) at ≥1 year. Left: Passive membrane properties assayed by current-clamp I/V demonstrated that all cells targeted exhibited inward rectification (WT n = 7, YAC128 n = 5). Middle: Dual eEPSCs (standard aCSF, +60 mV) shows increased relative eEPSC charge in YAC128 MSNs at high stimulus intensities only (WT n = 7, YAC128 n = 7). Right: Isolated NMDAR eEPSC (+60 mV, 10 μM CNQX) decay Tau_W before and after glutamate transport block (10 μM TBOA, 10 min) producing Ex-I_{NMDA} activity (ΔI_{NMDA} decay) that was significantly increased in YAC128s (WT n = 4, YAC128 n = 4, two-way RM ANOVAs, MW t tests).

(C) Electron Microscopy at 1 year. Left: Representative electron micrograph showing two striatal synapses and contacting astrocyte processes (bar = 500 nm, shaded: perisynaptic astrocyte processes, line: postsynaptic density delineated). Right: There were no differences in the proportion of synapses with astrocyte contacts per 100 μm^2 or the distance between the PSD and astrocytic processes between aged-matched wild-type littermates and YAC128 brains (WT n = 3 mice 92 synapses, YAC128 n = 3 mice 107 synapses).

Data expressed as mean ± SEM, except for the whisker box plots in (A).

DISCUSSION

Previous investigations in HD mice have demonstrated that mhtt expression alters NMDAR function from the earliest stages of disease (reviewed in Cepeda et al., 2007; Fan and Raymond, 2007). Some of the observed perturbations in NMDAR activity would be detrimental to neuronal function (Milnerwood et al., 2006; Milnerwood and Raymond, 2007; Milnerwood and Raymond, 2006; Murphy et al., 2000; Wolf et al., 2005) and adversely impact neuronal survival (Graham et al., 2006a, 2006b; Shehadeh et al., 2006; Zeron et al., 2002, 2004).

Here we demonstrate that NMDAR current in YAC128 MSNs is similar to WT and YAC18 controls when produced by low or moderate levels of synaptic activity, but increased at high levels. The NMDAR components of mEPSCs, large AP-dependent sEPSCs, and even low-stimulus-intensity eEPSCs were all similar between YAC128 and control mice. Elevations in YAC128 I_{NMDA} were only apparent with high levels of synchronously released glutamate from many synapses. Specifically, small increases were observed with high stimulation intensities (driving release from a large number of inputs), and large increases were revealed by paired stimuli driving facilitated release at many individual synapses. This suggests that spillover of glutamate to extrasynaptic sites is required to unmask augmented I_{NMDA} in YAC128 MSNs. In agreement with this, blockade of glutamate transporters and individual stimuli revealed similarly large increases in YAC128 I_{NMDA}. These results indicate that expression of full-length mhtt enhances NMDAR current outside synapses, shifting the balance of synaptic:extrasynaptic NMDAR activity.

Altered NMDAR Trafficking and Excitotoxicity

Elevated Ex-I_{NMDA} in YAC128 MSNs was abolished by NR2B-type NMDAR selective blockade, and although NR1, NR2A, and NR2B subunits all showed a shift from synaptic to nonsynaptic membranes, by far the largest effect was on NR2B subunits. Together the data strongly suggest that mhtt results in the expression of a distinct population of NR2B-containing extrasynaptic NMDARs. Although we have not addressed the mechanism of NMDAR mislocalization here, we have demonstrated elsewhere that calpain activity levels are elevated in YAC HD MSNs (Cowan et al., 2008). Calpain activity cleaves the C-terminal region of NR2B NMDAR subunits, resulting in functional membrane-bound receptors lacking regulatory

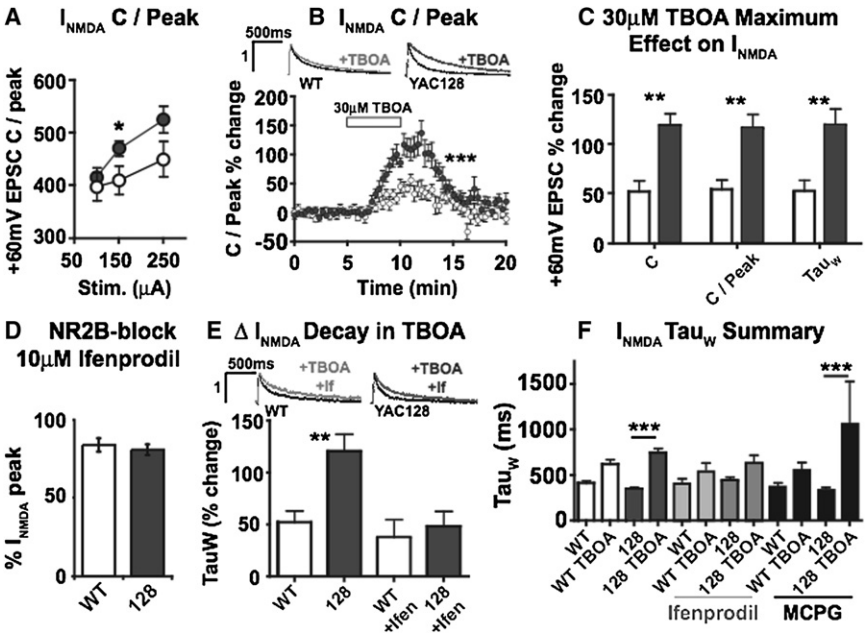

Figure 6. Ex-I_{NMDA} Is Not Due to Decreased Uptake and Is Mediated by NR2B Subunit-Containing NMDAR

(A) Dual eEPSCs (standard aCSF, +60 mV) show increased relative eEPSC charge in YAC128 MSNs at high stimulus intensities only (YAC128 n = 10 filled versus WT n = 13 clear).

(B) Transient exposure of isolated NMDAR eEPSCs (+60 mV, 10 μM CNQX) to 30 μM TBOA (5 min) produced Ex-I_{NMDA} activity (ΔI_{NMDA} relative charge) that was significantly greater in YAC128s (two-way RM AVOVA, WT n = 9 YAC128 n = 13).

(C) Summary of TBOA effects; percent changes in charge, relative charge, and decay Tau_W were significantly increased in YAC128 MSNs (two-way ANOVA, Bonferroni post hoc).

(D) Ifenprodil significantly reduced isolated NMDAR eEPSC peaks to an equal extent in both genotypes (WT n = 5, YAC128 n = 4).

(E) The increase in decay Tau_W produced by TBOA (group data as in top right) was not significantly different between genotypes in the presence of ifenprodil (10 μM, WT n = 3, YAC128 n = 4).

(F) Summary data of I_{NMDA} decay Tau_W before and during 30 μM TBOA alone or in the presence of ifenprodil (10 μM) or s-MCPG (250 μM WT n = 3 YAC128 n = 3, one-way ANOVA, Bonferroni post hoc).

Data expressed as mean ± SEM.

C-terminal tails (Wu et al., 2007) responsible for synaptic versus extrasynaptic localization (Prybylowski et al., 2005). Thus, elevated calpain activity may contribute to increased extrasynaptic (NR2B-containing) NMDARs.

Previous work demonstrates that HD striatal neurons in vivo and culture are more sensitive to NMDAR excitotoxicity. Intrastriatal injection of the NMDAR agonist quinolinic acid produces a significantly larger lesion in YAC128 versus WT mice at 3 months (Graham et al., 2006a), consistent with an increased proportion of extrasynaptic compared with synaptic activity in YAC128 striatum, as shown here. In neuronal culture, both YAC72 and YAC128 MSNs are hypersensitive to

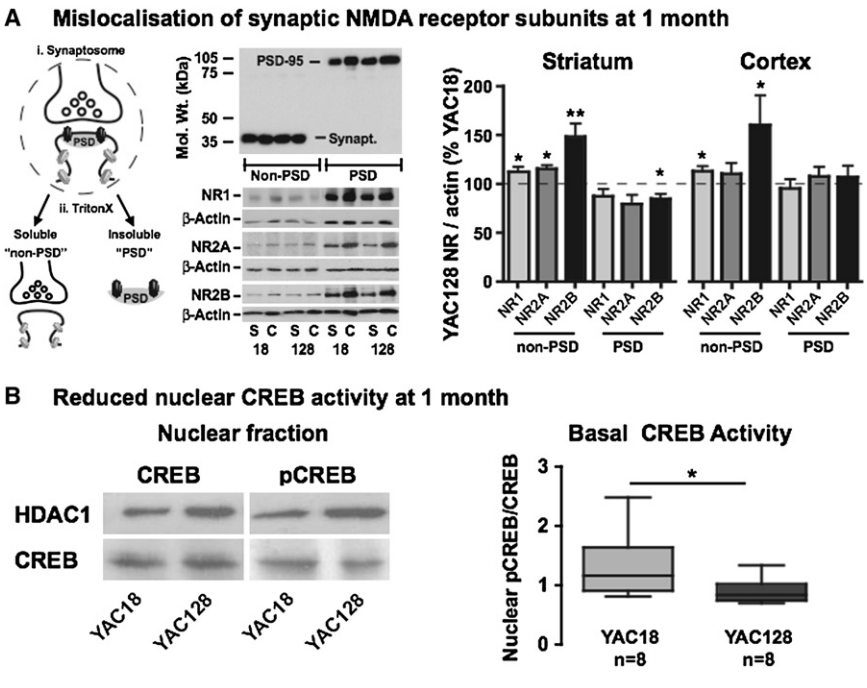

Figure 7. Altered NMDAR Subunit Localization and Reduced CREB Signaling

(A) Model of fractionation protocol; synaptosomes are digested to yield Triton-X-insoluble PSD-enriched (PSD) and -soluble non-PSD enriched (non-PSD) fractions, corresponding to synaptic versus peri-/extrasynaptic and presynaptic membranes (left). Representative blots showing separation of PSD and non-PSD fractions in striatal (S) and cortical (C) synaptosomes from YAC18 and YAC128 mice; as demonstrated by PSD-95 and synaptophysin separation (middle). Fractions were probed for NR1, NR2A, and NR2B subunit alterations in YAC128 mice (NR1 n = 10, NR2A n = 5, NR2B n = 11 relative to paired YAC18); NR1, NR2A, and NR2B subunit immunoreactivity (relative to actin) were significantly increased in non-PSD fractions from YAC128 striatum. Significant reductions in NR2B were also observed in striatal PSD "synaptic" fractions. NR1 and NR2B were also significantly elevated in non-PSD fractions from cortex, yet no alterations were observed in the PSD (Wilcoxon SR t test).

(B) Nuclear fractionation was confirmed by HDAC1 immunoreactivity and striatal samples were probed for CREB and pCREB (representative blots left). Basal CREB activation was significantly reduced in YAC128 striatum at 1 month (MW t test).

Data expressed as mean ± SEM (A) and whisker box plot (B).

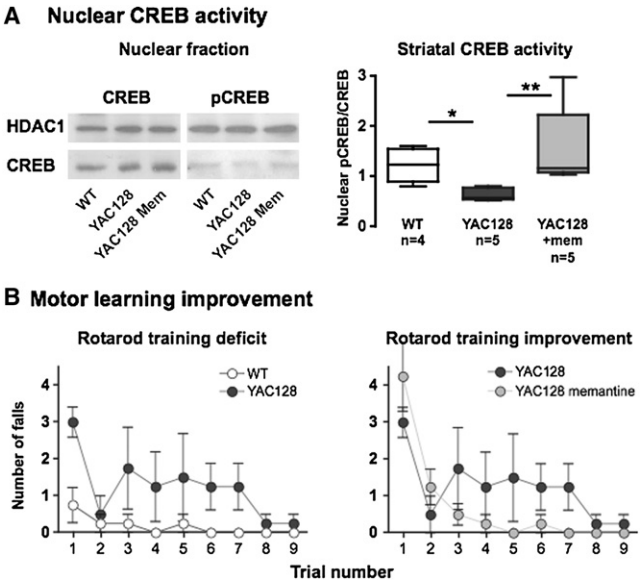

Figure 8. CREB Activation and Motor Learning Deficits Are Reversed by Memantine Treatment

(A) At 4 months, nuclear CREB activity (representative blots left) is significantly reduced in YAC128 striatum. Memantine treatment from 2 months significantly restored CREB activation to WT levels in YAC128 mice (right, one-way ANOVA $p = 0.015$, KW stat = 8.3, direct comparison t tests shown).

(B) At four months, YAC128 mice learn the rotarod task significantly slower than WT mice (left). Memantine-treated YAC128 mice exhibit significantly improved motor learning versus untreated YAC128s (two-way ANOVA interaction: WT versus YAC128 $p = 0.029$, $F_{8,48} = 2.4$, YAC128 versus YAC128-memantine $p = 0.0026$, $F_{8,48} = 3.6$).

Data expressed as whisker box plot (A) and mean ± SEM (B).

NMDAR-mediated apoptosis compared to WT or YAC18 MSNs (Graham et al., 2006b; Shehadeh et al., 2006; Tang et al., 2005; Zeron et al., 2002, 2004) and show increased NMDAR whole-cell current and/or toxic signaling (Fan et al., 2007; Fernandes et al., 2007; Zhang et al., 2008). In YAC128 MSNs, Ca^{2+} entry through NMDARs leads to enhanced mitochondrial depolarization, permeability transition, and consequently apoptosis (Fernandes et al., 2007; Shehadeh et al., 2006). Notably, studies in neuronal culture indicate that extrasynaptic NMDAR signaling triggers mitochondrial membrane potential breakdown and cell death (Hardingham et al., 2002; Leveille et al., 2008). Moreover, Leveille et al. (2008) and others (Stanika et al., 2009) demonstrate that high synaptic NMDAR activity does not produce cytosolic Ca^{2+} overload and produces no deleterious effects. It is likely that a greater proportion of extrasynaptic NMDAR transmission results in enhanced NMDA-induced toxicity in cultured YAC128 striatal MSNs.

Relevance of Extrasynaptic Transmission to Signaling Pathways Implicated in HD Pathogenesis

In brains from HD mice and human autopsy tissue, the neuronal survival factor BDNF is reduced (Fusco et al., 2003; Reilly, 2001; Zuccato et al., 2001, 2005), cysteine proteases known to cleave htt and contribute to cell death are upregulated (Gafni and Ellerby, 2002; Gafni et al., 2004; Goldberg et al., 1996; Wellington et al., 2002), mitochondria are dysfunctional, cellular energy levels are low (Panov et al., 2002; Panov et al., 2005; Seong et al., 2005), and gene transcription, particularly that mediated by CREB, is dysregulated (Cha, 2007; Gines et al., 2003; Sugars et al., 2004; Wyttenbach et al., 2001). Excessive extrasynaptic NMDAR activity would be predicted to contribute to all of these changes (Papadia and Hardingham, 2007).

In contrast to synaptic activity, extrasynaptic NMDAR signaling triggers "cell death" transcriptional signaling by suppressing phosphorylated (activated) CREB and failing to similarly activate ERK in hippocampal cells (Hardingham et al., 2002; Leveille et al., 2008). Indeed, we found that nuclear CREB activation was reduced in both 1 month and 4 month YAC128 mouse striatum, in agreement with a previous study showing reduced CREB phosphorylation and BDNF transcription at early stages in knockin HD mice (Gines et al., 2003). Strikingly, the reduction in CREB activity, along with associated motor learning deficits, found in YAC128 mice were reversed by treatment with a low dose of memantine, previously shown to selectively inhibit Ex-I_{NMDA} while preserving synaptic NMDAR current (Leveille et al., 2008; Okamoto et al., 2009; Papadia et al., 2008). Moreover, Okamoto and colleagues (Okamoto et al., 2009) demonstrated rescue of striatal volume loss and rotarod deficits at 12 months in YAC128 mice treated with low dose memantine, whereas a 30-fold higher dose, which should inhibit both synaptic and extrasynaptic NMDAR current, worsened the phenotype and neurodegeneration in YAC128 mice. Together with the results of that study, our observations at a very early, presymptomatic age in YAC128 mice suggest a key role for aberrant extrasynaptic NMDAR signaling in the onset of HD behavioral, motor, and neurodegenerative phenotypes.

In addition to the link between enhanced Ex-I_{NMDA} and reduced survival signaling via nuclear CREB activity in the YAC128 striatum, we have also shown that altered NMDAR localization and/or current is observed to a lesser extent in (1) mice expressing fewer repeats (YAC72) and a milder HD phenotype and (2) in the YAC128 cortex, a brain region affected later than the striatum in both human HD pathology (Vonsattel and DiFiglia, 1998) and YAC128 mice (Cummings et al., 2009; Slow et al., 2003). These data suggest that augmented extrasynaptic NMDAR activity is specific to conditions that lead to HD pathogenesis. Moreover, mhtt augmentation of Ex-I_{NMDA} was absent in C6R mice that express full-length mhtt, but are protected from the phenotypic and neuropathological effects of the transgene. This finding provides a firm link between mhtt-induced augmentation of Ex-I_{NMDA} signaling and HD pathogenesis and suggests that mhtt cleavage and toxic fragment formation are prerequisites for augmented Ex-I_{NMDA} (cell death signaling), phenotype, and neuropathology in YAC128 mice.

Activation of Extrasynaptic NMDA Receptors

Although the physiological role of extrasynaptic NMDAR transmission is debated, theories suggest that they constitute a reserve pool for synaptic receptors or belong to a distinct signaling pathway (reviewed in Köhr, 2006; and Lau and Zukin, 2007). Stimulated activity, modeling endogenous activity patterns, does activate extrasynaptic NR2B-containing NMDARs in the hippocampus (Lozovaya et al., 2004) and perirhinal cortex

(Massey et al., 2004). Furthermore, in retinal ganglion cells and cerebellar stellate cells that lack synaptic NMDARs, high stimulation intensities or facilitated release, such as those employed here, are required to activate perisynaptic NMDARs by spillover (Carter and Regehr, 2000; Chen and Diamond, 2002; Clark and Cull-Candy, 2002). The defining characteristics of striatal MSNs include a low resting membrane potential and a high level of excitatory input required to drive up-state transitions (predicted to be >1000 Hz) and action potential firing (Wilson and Kawaguchi, 1996; Wolf et al., 2005). Such high activity levels might render glutamatergic inputs to MSNs predisposed to spillover onto extrasynaptic sites, which may be pathological in YAC128 MSNs due to increased receptor numbers.

In MSNs of the nucleus accumbens, extrasynaptic NMDAR activity can also be driven by astrocytic glutamate release (D'Ascenzo et al., 2007), dependent upon the activation of glial mGluR5 receptors. As elevated extrasynaptic NMDAR activity in YAC128 MSNs persisted when mGluRs were blocked, our data suggest that this form of release was not engaged. However, as with YAC128 MSNs, extrasynaptic gliotransmission was blocked by the NR2B-subunit-selective antagonist ifenprodil (ibid). Thus, glial release is another candidate mechanism for the physiological activation of elevated extrasynaptic NMDARs in YAC128 MSNs. It follows that increased glutamate reuptake would lessen the magnitude of extrasynaptic NMDAR activation. Indeed, it has recently been shown that increasing glutamate uptake in HD mice reduces the behavioral phenotype (Miller et al., 2008). The question of how these receptors become activated in YAC128 MSNs will be the basis of future investigations.

Conclusions

Several studies have highlighted the adverse effects of extrasynaptic NMDAR signaling for neuronal viability in vitro (Gouix et al., 2009; Hardingham et al., 2002; Leveille et al., 2008; Okamoto et al., 2009; Papadia et al., 2008), and we present a direct link between an inherited neurodegenerative disease and elevated extrasynaptic NMDAR transmission. Others have shown that the clinically approved NMDAR antagonist memantine, likely because of its unusual pharmacodynamics (Parsons et al., 2007), specifically silences detrimental extrasynaptic NMDAR activity, while leaving beneficial synaptic signaling unaffected (Leveille et al., 2008; Okamoto et al., 2009; Papadia et al., 2008). In addition to a previous report that memantine treatment successfully reduced neuropathological and behavioral deficits in HD mice at late stages (Okamoto et al., 2009), the study presented here demonstrates that appropriate intervention can delay early signaling and behavioral deficits in HD mice. Thus, pharmacological mitigation of augmented extrasynaptic NMDAR activity, along with drugs that boost glutamate uptake, may delay onset and prevent progression of human HD.

EXPERIMENTAL PROCEDURES

Transgenic Mice and Brain Slice Preparation

YAC18, YAC72(2511), YAC128(55), C6R (W7 and W13), and YAC128(53)/WT littermate mice (Graham et al., 2006a; Hodgson et al., 1999; Slow et al., 2003) were maintained according to Canadian Council on Animal Care regulations at the UBC Faculty of Medicine Animal Resource Unit. Acute coronal slices were prepared for electrophysiological recording as in Milnerwood and Raymond (2007). In mice aged >1 year, parasagittal slices were prepared and the same striatal region targeted.

Electrophysiology

Basic methodology was as in Milnerwood and Raymond (2007). Standard artificial cerebrospinal fluid (aCSF) was identical excepting glycine (10 μM) and strychnine (2 μM) were added to augment NMDAR activity and block glycine receptors, respectively. Pipette resistance (Rp) was 3–6 MΩ when filled with (in mM) 130 Cs methanesulfonate, 5 CsCl, 4 NaCl, 1 $MgCl_2$, 5 EGTA, 10 HEPES, 5 QX-314, 0.5 GTP, 10 Na_2-phosphocreatine, and 5 MgATP, pH 7.3, 290–295 mOsM. Tolerance for series resistance (Rs) was <20 MΩ and uncompensated; ΔRs tolerance was <50% (mean change Rs = 10.2% ± 3.7%), providing Rs did not exceed 30 MΩ. Results were confirmed by repeated analysis and offline Rs compensation using AxographX. Recordings were made in 100 μM picrotoxin (PTX) to block $GABA_A$ receptors, and further bath application of AMPA/kainate receptor antagonist 10 μM 6-cyano-2,3-dihydroxy-7-nitro-quinoxaline (CNQX), 10 or 30 μM GLT1/EAAT2 blocker DL-threo-b-Benzyloxyaspartic acid (TBOA), and 50 μM NMDAR antagonist D-(-)-2-amino-5-phosphonopentanoic acid (D-AP5) or 5 μM NMDAR antagonist (+/−)-4-(trans)-2-carboxy-5,7-dichloro-4-phenylaminocarbonylamino -1,2,3,4- tetrahydroquinoline (L689,560) where stated (Tocris Bioscience, MO, USA). Signals were filtered at 2 kHz, digitized at 10 kHz, and analyzed in Clampfit10 (Axon Instruments, CA, USA).

sEPSCs were analyzed using Clampfit10 (threshold 8 pA). Individual cell cumulative probabilities were plotted by genotype mean ± SEM. eEPSCs were evoked by intrastriatal stimulation (100–200 μs) via micropipettes (2–5 MΩ in aCSF) 150–200 μm dorsally. Concomitant field recording was performed at the same depth, 50–100 μm, of the target cell. Evoked currents are averages of three (0.066 Hz); kinetics expressed as Tau (t) or tau weighted (t_W) following Stocca and Vicini (1998).

I_{NMDA} was isolated by (1) dual AMPA and NMDA receptor-mediated currents in modified aCSF (standard aCSF excepting: 5 μM Mg^{2+}, 20 μM glycine, 2 μM strychnine; "Low Mg^{2+}"), prior to D-AP5 or L689560 to produce subtracted I_{NMDA} (Thomas et al., 2000); (2) in standard aCSF, cells were depolarized to −20 (sEPSCs) or +60 mV (eEPSCs) to relieve voltage-dependent Mg^{2+} block prior to isolation by CNQX or D-AP5 block. After >3 min baseline, TBOA was added and responses tracked for 5 or >10 min, prior to washout or AP5 addition. In addition to VC, IC recordings were conducted in aged mouse slices using K^+-gluconate ICS (129.4 K^+-gluconate, 11.1 KCl, 4 NaCl, 0.02 EGTA, 10 HEPES, 0.3 GTP, and 3 MgATP, pH 7.3, 290–295 mOsM). Results are mean ± SEM. Significance was tested in GraphPad Prism (La Jolla, CA, USA).

Golgi Impregnation and Cell Reconstruction

YAC18 (n = 4) and YAC128 (n = 4) mice were pentobarbital anesthetized then perfused with 0.9% sucrose prior to Golgi-Cox impregnation (see Supplemental Experimental Procedures). MSNs were manually reconstructed (drawn through ×40 z stacks) and spine densities calculated by visual identification of spines in higher magnification overlays (×100 z stacks) using custom software routines for Igor Pro (Wavemetrics; Lake Oswego, Oregon) designed in house by J.D.B. as in Brown et al. (2007).

Electron Microscopy

Tissue for electron microscopy was harvested and prepared as in Hines et al. (2008). For details, see Supplemental Experimental Procedures.

Tissue Preparation, Subcellular Fractionation, and Western Blot Analyses

Subcellular fractionation was conducted on tissue from P23–P38 (YAC18, 29.5 ± 1.5 and YAC128, 31.2 ± 1.7) mice using an adapted protocol (Pacchioni et al., 2009). Tissue was paired by day of dissection. Nuclear fractionation was performed on tissue from 4-month-old brains. For details see Supplemental Experimental Procedures.

Memantine Treatment

YAC128 mice (n = 10) and WT littermate mice (n = 4) were housed in identical conditions. At 2 months, half the YAC128 mice (n = 5) were treated with 1 mg/kg memantine (Sigma) in drinking water (Okamoto et al., 2009). Mice

were subjected to rotarod training (Van Raamsdonk et al., 2005) prior to perfusion, then brains were microdissected and flash frozen prior to tissue preparation. For details, see Supplemental Experimental Procedures.

SUPPLEMENTAL INFORMATION

Supplemental Information includes Supplemental Experimental Procedures, four figures, and one table and can be found with this article online at doi:10.1016/j.neuron.2010.01.008.

ACKNOWLEDGMENTS

We wish to thank A. George, T. Okbinoglu, and K. Duthie for excellent technical support; Dr. C. Brown for guidance with histology; Drs. P. Kalivas and A. Pacchioni for the synaptosome fractionation; and Dr C. Taghibiglou and S Zhang for the nuclear fractionation. The study was supported by grants from the Canadian Institutes of Health Research (CIHR MOP-12699), Michael Smith Foundation for Health Research (MSFHR), and the Heart & Stroke Foundation of BC & Yukon. A.J.M. was a Bluma Tischler Fellowship and CIHR Fellowship awardee and held a joint Fellowship from the Huntington's Disease Society of America and Huntington Society Canada while this work was conducted. L.A.R. held MSFHR Senior Scholar and CIHR Investigator awards. M.R.H is a University Killam Professor and holds a Canada Research Chair in Human Genetics. The research was designed by A.J.M. and L.A.R. with input from T.H.M. All electrophysiology experiments were conducted by A.J.M. with contribution from O.C.V. C.M.G. performed biochemical fractionation and immunoblotting with assistance of R.W.Y.K. M.A.P. provided the memantine-treated mouse cohort and performed behavioral testing. A.M.K. and A.J.M. conducted Golgi and 3D cell-reconstruction with tools and guidance from J.D.B. R.M.H. produced EM studies. M.R.H. and R.K.G. contributed reagents and advice. A.J.M. wrote the manuscript with direction from L.A.R. All authors contributed to editing.

Accepted: December 29, 2009
Published: January 27, 2010

REFERENCES

Andre, V.M., Cepeda, C., Venegas, A., Gomez, Y., and Levine, M.S. (2006). Altered cortical glutamate receptor function in the R6/2 model of Huntington's disease. J. Neurophysiol. *93*, 2108–2119.

Arnth-Jensen, N., Jabaudon, D., and Scanziani, M. (2002). Cooperation between independent hippocampal synapses is controlled by glutamate uptake. Nat. Neurosci. *5*, 325–331.

Arundine, M., and Tymianski, M. (2003). Molecular mechanisms of calcium-dependent neurodegeneration in excitotoxicity. Cell Calcium *34*, 325–337.

Bliss, T.V.P., and Collingridge, G.L. (1993). A synaptic model of memory: long-term potentiation in the hippocampus. Nature *361*, 31–39.

Brown, C.E., Li, P., Boyd, J.D., Delaney, K.R., and Murphy, T.H. (2007). Extensive turnover of dendritic spines and vascular remodeling in cortical tissues recovering from stroke. J. Neurosci. *27*, 4101–4109.

Carter, A.G., and Regehr, W.G. (2000). Prolonged synaptic currents and glutamate spillover at the parallel fiber to stellate cell synapse. J. Neurosci. *20*, 4423–4434.

Cepeda, C., Ariano, M.A., Calvert, C.R., Flores-Hernández, J., Chandler, S.H., Leavitt, B.R., Hayden, M.R., and Levine, M.S. (2001a). NMDA receptor function in mouse models of Huntington disease. J. Neurosci. Res. *66*, 525–539.

Cepeda, C., Hurst, R.S., Altemus, K.L., Flores-Hernández, J., Calvert, C.R., Jokel, E.S., Grandy, D.K., Low, M.J., Rubinstein, M., Ariano, M.A., and Levine, M.S. (2001b). Facilitated glutamatergic transmission in the striatum of D2 dopamine receptor-deficient mice. J. Neurophysiol. *85*, 659–670.

Cepeda, C., Wu, N., André, V.M., Cummings, D.M., and Levine, M.S. (2007). The corticostriatal pathway in Huntington's disease. Prog. Neurobiol. *81*, 253–271.

Cha, J.H. (2007). Transcriptional signatures in Huntington's disease. Prog. Neurobiol. *83*, 228–248.

Chen, S., and Diamond, J.S. (2002). Synaptically released glutamate activates extrasynaptic NMDA receptors on cells in the ganglion cell layer of rat retina. J. Neurosci. *22*, 2165–2173.

Chen, H.S., and Lipton, S.A. (2006). The chemical biology of clinically tolerated NMDA receptor antagonists. J. Neurochem. *97*, 1611–1626.

Clark, B.A., and Cull-Candy, S.G. (2002). Activity-dependent recruitment of extrasynaptic NMDA receptor activation at an AMPA receptor-only synapse. J. Neurosci. *22*, 4428–4436.

Cowan, C.M., and Raymond, L.A. (2006). Selective neuronal degeneration in Huntington's disease. Curr. Top. Dev. Biol. *75*, 25–71.

Cowan, C.M., Fan, M.M., Fan, J., Shehadeh, J., Zhang, L.Y., Graham, R.K., Hayden, M.R., and Raymond, L.A. (2008). Polyglutamine-modulated striatal calpain activity in YAC transgenic huntington disease mouse model: impact on NMDA receptor function and toxicity. J. Neurosci. *28*, 12725–12735.

Cummings, D.M., André, V.M., Uzgil, B.O., Gee, S.M., Fisher, Y.E., Cepeda, C., and Levine, M.S. (2009). Alterations in cortical excitation and inhibition in genetic mouse models of Huntington's disease. J. Neurosci. *29*, 10371–10386.

D'Ascenzo, M., Fellin, T., Terunuma, M., Revilla-Sanchez, R., Meaney, D.F., Auberson, Y.P., Moss, S.J., and Haydon, P.G. (2007). mGluR5 stimulates gliotransmission in the nucleus accumbens. Proc. Natl. Acad. Sci. USA *104*, 1995–2000.

Ding, J., Peterson, J.D., and Surmeier, D.J. (2008). Corticostriatal and thalamostriatal synapses have distinctive properties. J. Neurosci. *28*, 6483–6492.

Duff, K., Paulsen, J.S., Beglinger, L.J., Langbehn, D.R., and Stout, J.C. (2007). Psychiatric symptoms in Huntington's disease before diagnosis: The Predict-HD study. Biol. Psychiatr. *62*, 1341–1346.

Fan, M.M., and Raymond, L.A. (2007). N-methyl-D-aspartate (NMDA) receptor function and excitotoxicity in Huntington's disease. Prog. Neurobiol. *81*, 272–293.

Fan, M.M., Fernandes, H.B., Zhang, L.Y., Hayden, M.R., and Raymond, L.A. (2007). Altered NMDA receptor trafficking in a yeast artificial chromosome transgenic mouse model of Huntington's disease. J. Neurosci. *27*, 3768–3779.

Fernandes, H.B., Baimbridge, K.G., Church, J., Hayden, M.R., and Raymond, L.A. (2007). Mitochondrial sensitivity and altered calcium handling underlie enhanced NMDA-induced apoptosis in YAC128 model of Huntington's disease. J. Neurosci. *27*, 13614–13623.

Fusco, F.R., Zuccato, C., Tartari, M., Martorana, A., De March, Z., Giampà, C., Cattaneo, E., and Bernardi, G. (2003). Co-localization of brain-derived neurotrophic factor (BDNF) and wild-type huntingtin in normal and quinolinic acid-lesioned rat brain. Eur. J. Neurosci. *18*, 1093–1102.

Gafni, J., and Ellerby, L.M. (2002). Calpain activation in Huntington's disease. J. Neurosci. *22*, 4842–4849.

Gafni, J., Hermel, E., Young, J.E., Wellington, C.L., Hayden, M.R., and Ellerby, L.M. (2004). Inhibition of calpain cleavage of huntingtin reduces toxicity: accumulation of calpain/caspase fragments in the nucleus. J. Biol. Chem. *279*, 20211–20220.

Gines, S., Seong, I.S., Fossale, E., Ivanova, E., Trettel, F., Gusella, J.F., Wheeler, V.C., Persichetti, F., and MacDonald, M.E. (2003). Specific progressive cAMP reduction implicates energy deficit in presymptomatic Huntington's disease knock-in mice. Hum. Mol. Genet. *12*, 497–508.

Glykys, J., and Mody, I. (2007). The main source of ambient GABA responsible for tonic inhibition in the mouse hippocampus. J. Physiol. *582*, 1163–1178.

Goldberg, Y.P., Nicholson, D.W., Rasper, D.M., Kalchman, M.A., Koide, H.B., Graham, R.K., Bromm, M., Kazemi-Esfarjani, P., Thornberry, N.A., Vaillancourt, J.P., and Hayden, M.R. (1996). Cleavage of huntingtin by apopain, a proapoptotic cysteine protease, is modulated by the polyglutamine tract. Nat. Genet. *13*, 442–449.

Gouix, E., Léveillé, F., Nicole, O., Melon, C., Had-Aissouni, L., and Buisson, A. (2009). Reverse glial glutamate uptake triggers neuronal cell death through extrasynaptic NMDA receptor activation. Mol. Cell. Neurosci. *40*, 463–473.

Graham, R.K., Deng, Y., Slow, E.J., Haigh, B., Bissada, N., Lu, G., Pearson, J., Shehadeh, J., Bertram, L., Murphy, Z., et al. (2006a). Cleavage at the caspase-6 site is required for neuronal dysfunction and degeneration due to mutant huntingtin. Cell *125*, 1179–1191.

Graham, R.K., Slow, E.J., Deng, Y., Bissada, N., Lu, G., Pearson, J., Shehadeh, J., Leavitt, B.R., Raymond, L.A., and Hayden, M.R. (2006b). Levels of mutant huntingtin influence the phenotypic severity of Huntington disease in YAC128 mouse models. Neurobiol. Dis. *21*, 444–455.

Hardingham, G.E., and Bading, H. (2003). The Yin and Yang of NMDA receptor signalling. Trends Neurosci. *26*, 81–89.

Hardingham, G.E., Fukunaga, Y., and Bading, H. (2002). Extrasynaptic NMDARs oppose synaptic NMDARs by triggering CREB shut-off and cell death pathways. Nat. Neurosci. *5*, 405–414.

Heng, M.Y., Detloff, P.J., Wang, P.L., Tsien, J.Z., and Albin, R.L. (2009). In vivo evidence for NMDA receptor-mediated excitotoxicity in a murine genetic model of Huntington disease. J. Neurosci. *29*, 3200–3205.

Hines, R.M., Wu, L., Hines, D.J., Steenland, H., Mansour, S., Dahlhaus, R., Singaraja, R.R., Cao, X., Sammler, E., Hormuzdi, S.G., et al. (2008). Synaptic imbalance, stereotypies, and impaired social interactions in mice with altered neuroligin 2 expression. J. Neurosci. *28*, 6055–6067.

Hodgson, J.G., Agopyan, N., Gutekunst, C.A., Leavitt, B.R., LePiane, F., Singaraja, R., Smith, D.J., Bissada, N., McCutcheon, K., Nasir, J., et al. (1999). A YAC mouse model for Huntington's disease with full-length mutant huntingtin, cytoplasmic toxicity, and selective striatal neurodegeneration. Neuron *23*, 181–192.

Köhr, G. (2006). NMDA receptor function: subunit composition versus spatial distribution. Cell Tissue Res. *326*, 439–446.

Lau, C.G., and Zukin, R.S. (2007). NMDA receptor trafficking in synaptic plasticity and neuropsychiatric disorders. Nat. Rev. Neurosci. *8*, 413–426.

Le Meur, K., Galante, M., Angulo, M.C., and Audinat, E. (2007). Tonic activation of NMDA receptors by ambient glutamate of non-synaptic origin in the rat hippocampus. J. Physiol. *580*, 373–383.

Leveille, F., El Gaamouch, F., Gouix, E., Lecocq, M., Lobner, D., Nicole, O., and Buisson, A. (2008). Neuronal viability is controlled by a functional relation between synaptic and extrasynaptic NMDA receptors. Faseb J. *22*, 4258–4271.

Li, L., Murphy, T.H., Hayden, M.R., and Raymond, L.A. (2004). Enhanced striatal NR2B-containing N-methyl-D-aspartate receptor-mediated synaptic currents in a mouse model of Huntington disease. J. Neurophysiol. *92*, 2738–2746.

Lozovaya, N.A., Grebenyuk, S.E., Tsintsadze, T.Sh., Feng, B., Monaghan, D.T., and Krishtal, O.A. (2004). Extrasynaptic NR2B and NR2D subunits of NMDA receptors shape 'superslow' afterburst EPSC in rat hippocampus. J. Physiol. *558*, 451–463.

Massey, P.V., Johnson, B.E., Moult, P.R., Auberson, Y.P., Brown, M.W., Molnar, E., Collingridge, G.L., and Bashir, Z.I. (2004). Differential roles of NR2A and NR2B-containing NMDA receptors in cortical long-term potentiation and long-term depression. J. Neurosci. *24*, 7821–7828.

Miller, B.R., Dorner, J.L., Shou, M., Sari, Y., Barton, S.J., Sengelaub, D.R., Kennedy, R.T., and Rebec, G.V. (2008). Up-regulation of GLT1 expression increases glutamate uptake and attenuates the Huntington's disease phenotype in the R6/2 mouse. Neuroscience *153*, 329–337.

Milnerwood, A.J., and Raymond, L.A. (2006). Synaptic Abnormalities Associated with Huntington's disease. In Molecular Mechanisms of Synaotogenesis, A. El-Husseini and A. Dityatev, eds. (New York: Springer), pp. 457–469.

Milnerwood, A.J., and Raymond, L.A. (2007). Corticostriatal synaptic function in mouse models of Huntington's disease: early effects of huntingtin repeat length and protein load. J. Physiol. *585*, 817–831.

Milnerwood, A.J., Cummings, D.M., Dallérac, G.M., Brown, J.Y., Vatsavayai, S.C., Hirst, M.C., Rezaie, P., and Murphy, K.P. (2006). Early development of aberrant synaptic plasticity in a mouse model of Huntington's disease. Hum. Mol. Genet. *15*, 1690–1703.

Murphy, K.P.S.J., Carter, R.J., Lione, L.A., Mangiarini, L., Mahal, A., Bates, G.P., Dunnett, S.B., and Morton, A.J. (2000). Abnormal synaptic plasticity and impaired spatial cognition in mice transgenic for exon 1 of the human Huntington's disease mutation. J. Neurosci. *20*, 5115–5123.

Okamoto, S., Pouladi, M.A., Talantova, M., Yao, D., Xia, P., Ehrnhoefer, D.E., Zaidi, R., Clemente, A., Kaul, M., Graham, R.K., et al. (2009). Balance between synaptic versus extrasynaptic NMDA receptor activity influences inclusions and neurotoxicity of mutant huntingtin. Nat. Med. *15*, 1407–1413.

Pacchioni, A.M., Vallone, J., Worley, P.F., and Kalivas, P.W. (2009). Neuronal pentraxins modulate cocaine-induced neuroadaptations. J. Pharmacol. Exp. Ther. *328*, 183–192.

Panov, A.V., Gutekunst, C.A., Leavitt, B.R., Hayden, M.R., Burke, J.R., Strittmatter, W.J., and Greenamyre, J.T. (2002). Early mitochondrial calcium defects in Huntington's disease are a direct effect of polyglutamines. Nat. Neurosci. *5*, 731–736.

Panov, A.V., Lund, S., and Greenamyre, J.T. (2005). Ca2+-induced permeability transition in human lymphoblastoid cell mitochondria from normal and Huntington's disease individuals. Mol. Cell. Biochem. *269*, 143–152.

Papadia, S., and Hardingham, G.E. (2007). The dichotomy of NMDA receptor signaling. Neuroscientist *13*, 572–579.

Papadia, S., Soriano, F.X., Léveillé, F., Martel, M.A., Dakin, K.A., Hansen, H.H., Kaindl, A., Sifringer, M., Fowler, J., Stefovska, V., et al. (2008). Synaptic NMDA receptor activity boosts intrinsic antioxidant defenses. Nat. Neurosci. *11*, 476–487.

Parsons, C.G., Stöffler, A., and Danysz, W. (2007). Memantine: a NMDA receptor antagonist that improves memory by restoration of homeostasis in the glutamatergic system—too little activation is bad, too much is even worse. Neuropharmacology *53*, 699–723.

Pouladi, M.A., Graham, R.K., Karasinska, J.M., Xie, Y., Santos, R.D., Petersén, A., and Hayden, M.R. (2009). Prevention of depressive behaviour in the YAC128 mouse model of Huntington disease by mutation at residue 586 of huntingtin. Brain *132*, 919–932.

Prybylowski, K., Chang, K., Sans, N., Kan, L., Vicini, S., and Wenthold, R.J. (2005). The synaptic localization of NR2B-containing NMDA receptors is controlled by interactions with PDZ proteins and AP-2. Neuron *47*, 845–857.

Reilly, C.E. (2001). Wild-type huntingtin up-regulates BDNF transcription in Huntington's disease. J. Neurol. *248*, 920–922.

Scimemi, A., Fine, A., Kullmann, D.M., and Rusakov, D.A. (2004). NR2B-containing receptors mediate cross talk among hippocampal synapses. J. Neurosci. *24*, 4767–4777.

Seong, I.S., Ivanova, E., Lee, J.M., Choo, Y.S., Fossale, E., Anderson, M., Gusella, J.F., Laramie, J.M., Myers, R.H., Lesort, M., and MacDonald, M.E. (2005). HD CAG repeat implicates a dominant property of huntingtin in mitochondrial energy metabolism. Hum. Mol. Genet. *14*, 2871–2880.

Sergueeva, O.A., Fedorov, N.B., and Reymann, K.G. (1993). An antagonist of glutamate metabotropic receptors, (RS)-alpha-methyl-4-carboxyphenylglycine, prevents the LTP-related increase in postsynaptic AMPA sensitivity in hippocampal slices. Neuropharmacology *32*, 933–935.

Shehadeh, J., Fernandes, H.B., Zeron Mullins, M.M., Graham, R.K., Leavitt, B.R., Hayden, M.R., and Raymond, L.A. (2006). Striatal neuronal apoptosis is preferentially enhanced by NMDA receptor activation in YAC transgenic mouse model of Huntington disease. Neurobiol. Dis. *21*, 392–403.

Slow, E.J., van Raamsdonk, J., Rogers, D., Coleman, S.H., Graham, R.K., Deng, Y., Oh, R., Bissada, N., Hossain, S.M., Yang, Y.Z., et al. (2003). Selective striatal neuronal loss in a YAC128 mouse model of Huntington disease. Hum. Mol. Genet. *12*, 1555–1567.

Smeal, R.M., Keefe, K.A., and Wilcox, K.S. (2008). Differences in excitatory transmission between thalamic and cortical afferents to single spiny efferent neurons of rat dorsal striatum. Eur. J. Neurosci. *28*, 2041–2052.

Solomon, A.C., Stout, J.C., Johnson, S.A., Langbehn, D.R., Aylward, E.H., Brandt, J., Ross, C.A., Beglinger, L., Hayden, M.R., Kieburtz, K., and , et al. Predict-HD investigators of the Huntington Study Group. (2007). Verbal

episodic memory declines prior to diagnosis in Huntington's disease. Neuropsychologia *45*, 1767–1776.

Stanika, R.I., Pivovarova, N.B., Brantner, C.A., Watts, C.A., Winters, C.A., and Andrews, S.B. (2009). Coupling diverse routes of calcium entry to mitochondrial dysfunction and glutamate excitotoxicity. Proc. Natl. Acad. Sci. USA *106*, 9854–9859.

Stocca, G., and Vicini, S. (1998). Increased contribution of NR2A subunit to synaptic NMDA receptors in developing rat cortical neurons. J. Physiol. *507*, 13–24.

Sugars, K.L., Brown, R., Cook, L.J., Swartz, J., and Rubinsztein, D.C. (2004). Decreased cAMP response element-mediated transcription: an early event in exon 1 and full-length cell models of Huntington's disease that contributes to polyglutamine pathogenesis. J. Biol. Chem. *279*, 4988–4999.

Tang, T.S., Slow, E., Lupu, V., Stavrovskaya, I.G., Sugimori, M., Llinás, R., Kristal, B.S., Hayden, M.R., and Bezprozvanny, I. (2005). Disturbed Ca2+ signaling and apoptosis of medium spiny neurons in Huntington's disease. Proc. Natl. Acad. Sci. USA *102*, 2602–2607.

Thomas, M.J., Malenka, R.C., and Bonci, A. (2000). Modulation of long-term depression by dopamine in the mesolimbic system. J. Neurosci. *20*, 5581–5586.

Tzingounis, A.V., and Wadiche, J.I. (2007). Glutamate transporters: confining runaway excitation by shaping synaptic transmission. Nat. Rev. Neurosci. *8*, 935–947.

Van Raamsdonk, J.M., Pearson, J., Slow, E.J., Hossain, S.M., Leavitt, B.R., and Hayden, M.R. (2005). Cognitive dysfunction precedes neuropathology and motor abnormalities in the YAC128 mouse model of Huntington's disease. J. Neurosci. *25*, 4169–4180.

Vonsattel, J.P., and DiFiglia, M. (1998). Huntington disease. J. Neuropathol. Exp. Neurol. *57*, 369–384.

Wellington, C.L., Leavitt, B.R., and Hayden, M.R. (2000). Huntington disease: new insights on the role of huntingtin cleavage. J. Neural Transm. Suppl., 1–17.

Wellington, C.L., Ellerby, L.M., Gutekunst, C.A., Rogers, D., Warby, S., Graham, R.K., Loubser, O., van Raamsdonk, J., Singaraja, R., Yang, Y.Z., et al. (2002). Caspase cleavage of mutant huntingtin precedes neurodegeneration in Huntington's disease. J. Neurosci. *22*, 7862–7872.

Whittaker, V.P. (1993). Thirty years of synaptosome research. J. Neurocytol. *22*, 735–742.

Williams, K. (2001). Ifenprodil, a novel NMDA receptor antagonist: site and mechanism of action. Curr. Drug Targets *2*, 285–298.

Wilson, C.J., and Kawaguchi, Y. (1996). The origins of two-state spontaneous membrane potential fluctuations of neostriatal spiny neurons. J. Neurosci. *16*, 2397–2410.

Wolf, J.A., Moyer, J.T., Lazarewicz, M.T., Contreras, D., Benoit-Marand, M., O'Donnell, P., and Finkel, L.H. (2005). NMDA/AMPA ratio impacts state transitions and entrainment to oscillations in a computational model of the nucleus accumbens medium spiny projection neuron. J. Neurosci. *25*, 9080–9095.

Wu, H.Y., Hsu, F.C., Gleichman, A.J., Baconguis, I., Coulter, D.A., and Lynch, D.R. (2007). Fyn-mediated phosphorylation of NR2B Tyr-1336 controls calpain-mediated NR2B cleavage in neurons and heterologous systems. J. Biol. Chem. *282*, 20075–20087.

Wyttenbach, A., Swartz, J., Kita, H., Thykjaer, T., Carmichael, J., Bradley, J., Brown, R., Maxwell, M., Schapira, A., Orntoft, T.F., et al. (2001). Polyglutamine expansions cause decreased CRE-mediated transcription and early gene expression changes prior to cell death in an inducible cell model of Huntington's disease. Hum. Mol. Genet. *10*, 1829–1845.

Zeron, M.M., Hansson, O., Chen, N., Wellington, C.L., Leavitt, B.R., Brundin, P., Hayden, M.R., and Raymond, L.A. (2002). Increased sensitivity to N-methyl-D-aspartate receptor-mediated excitotoxicity in a mouse model of Huntington's disease. Neuron *33*, 849–860.

Zeron, M.M., Fernandes, H.B., Krebs, C., Shehadeh, J., Wellington, C.L., Leavitt, B.R., Baimbridge, K.G., Hayden, M.R., and Raymond, L.A. (2004). Potentiation of NMDA receptor-mediated excitotoxicity linked with intrinsic apoptotic pathway in YAC transgenic mouse model of Huntington's disease. Mol. Cell. Neurosci. *25*, 469–479.

Zhang, H., Li, Q., Graham, R.K., Slow, E., Hayden, M.R., and Bezprozvanny, I. (2008). Full length mutant huntingtin is required for altered Ca2+ signaling and apoptosis of striatal neurons in the YAC mouse model of Huntington's disease. Neurobiol. Dis. *31*, 80–88.

Zuccato, C., Ciammola, A., Rigamonti, D., Leavitt, B.R., Goffredo, D., Conti, L., MacDonald, M.E., Friedlander, R.M., Silani, V., Hayden, M.R., et al. (2001). Loss of huntingtin-mediated BDNF gene transcription in Huntington's disease. Science *293*, 493–498.

Zuccato, C., Liber, D., Ramos, C., Tarditi, A., Rigamonti, D., Tartari, M., Valenza, M., and Cattaneo, E. (2005). Progressive loss of BDNF in a mouse model of Huntington's disease and rescue by BDNF delivery. Pharmacol. Res. *52*, 133–139.